

The magnetic properties dependence on temperature of Li-ferrite nanoparticle

M. H. Al-Dharob^a, I. M. Abdulmajeed^{b,*}, A. H. Taha^c, E. K. AL-Shakarchi^d,
B. Elouadi^e

^aAl-Karkh University of science/ Department of registrations / Baghdad / Iraq/

^bUniversity of Baghdad/ College of Science / Department of Physics / Baghdad /
Iraq

^cKoya University/ Faculty of Science and Health/ Department of
Physics/ Kurdistan region/ Iraq

^dAl-Nahrain University/ College of Science / Department of Physics / Baghdad /
Iraq

^ePolyscience and Technology/ La Rochelle University/ La Rochelle / France/

The chemical formula $\text{Li}_{0.5}\text{Fe}_{2.5}\text{O}_4$ of lithium ferrite prepared by two different chemical methods mentioned as low temperature solid state reaction (LTSSR) and modified combustion method (MCM). The samples showed nanoparticle scale with spinal structure. The magnetic analyses have done by the vibrating sample magnetometer VSM device, and both samples have the same magnetic properties represented by the magnetic saturation, remanence magnetization, and coercive magnetic field. The shape of hysteresis loop showed a soft ferrite and its area decreased with temperature increasing. On the other hand, the magnetic susceptibility decreased with increasing temperature for both samples of ferrite $\text{Li}_{0.5}\text{Fe}_{2.5}\text{O}_4$ prepared. The sample of LTSSR exhibited a magnetic moment of about $0.4 \times 10^{-3} \text{ JT}^{-1}$ at applied magnetic field 50 kOe which is approaching the same for the sample prepared by MCM method.

(Received November 11, 2021; Accepted February 11, 2022)

Keywords: Ferrite materials, Low temperature solid state reaction, Modified combustion method, Magnetic susceptibility, Magnetic moments

1. Introduction

Ferrite becomes one of the interested magnetic materials that applied in wide range of frequencies, its structure is a switching key to the electric, magnetic properties and supporting an important role in technological applications. A ferrite has three phases, one of them is a cubic spinel structure with the general formula $\text{MO} \cdot \text{Fe}_2\text{O}_3$ such as ($\text{M}=\text{Mn}^{+2}, \text{Fe}^{+2}, \text{Co}^{+2}, \text{Ni}^{+2}, \text{Cu}^{+2}, \text{Zn}^{+2}, \text{Mg}^{+2}$), the second one is a hexagonal ferrite with the formula $\text{MO} \cdot 6\text{Fe}_2\text{O}_3$ ($\text{M}=\text{Ba}^{+2}, \text{Ca}^{+2}, \text{Sr}^{+2}$), and the last one is a garnet formula $2\text{M}_2\text{O}_3 \cdot 5\text{Fe}_2\text{O}_3$, M is a cation of rare earth element with (+3) valence like Y [1]. The lithium ferrite LiFe_5O_8 is a cubic spinel structure [2]. It is belong to a soft ferrite material at a Curie temperature in a range (620°C) [3], a square hysteresis loop and high saturation magnetization. For this reason, it was designed for microwave devices and memory core applications. Lithium ferrite is an inverse spinel structure, which exists in two crystalline shapes; ordered $\alpha\text{-Li}_{0.5}\text{Fe}_{2.5}\text{O}_4$, and disordered $\beta\text{-Li}_{0.5}\text{Fe}_{2.5}\text{O}_4$ [4,5]. The β -phase has a tetrahedral site occupied by Fe^{+3} and randomly distributed over the octahedral sites. The α -phase with a space group $\text{P}_4132/\text{P}_4332$ called an order spinel phase. It had octahedral and tetrahedral sites occupied by Fe^{+3} ions in a primitive unit cell, and the octahedral positions occupied by Li^{+1} ions [6]. The $\beta\text{-LiFe}_5\text{O}_8$ has $\text{Fd}3\text{m}$ space group as disordered phase, it was obtained via the quenching from temperatures higher than (800°C) to room temperature. Ordered phase of lithium ferrite obtained at slow cooling temperature at about 750°C [7]. The different preparation methods used to prepare ferrite, such as low temperature solid state reaction (LTSSR) and modified combustion method

* Corresponding author: inaam.mohammed@sc.uobaghdad.edu.iq
<https://doi.org/10.15251/DJNB.2022.171.201>

(MCM). They supported many important parameters on magnetic properties [8, 9-12]. A Wide application of such kind of spinel ferrites with high frequency zone operating and Snoek limitation with tight band width [13-15]. The reports of ferrite nanoparticles are a suitable to a new biomedical technologies like high-density magnetic storage, magnetic transport for drug delivery, and high resolution of magnetic resonance imaging. The ferrite nanoparticles exhibited abnormal magnetic behavior that is unfamiliar a bulk material mentioned by a single domain property, superparamagnetic, and low magnetized [16,17]. The superparamagnetic is a unique and important feature in the ferrite nanoparticles. The Li-ferrite nanoparticles investigated previously [8], they showed the presence of pure phase of Li-ferrite prepared by two different methods, and both procedure showed a fine particle of about (46-77 nm). The unusual magnetic behavior at the low magnetic field called as negative magnetization [18-20]. This paper dealing with the explanation more information about the effect of preparation methods and temperature on the behavior of Li-Ferrite nanoparticle

2. Experiment procedure

The synthesis of Li-ferrite powder had been done by two chemical procedures as mentioned before [8]. These chemical methods produced stoichiometry magnetic compounds. They considered a source of Fe^{+3} ions because the presence of chlorine in all starting materials, such that $\text{LiCl}\cdot\text{H}_2\text{O}$, $\text{NiCl}_2\cdot 6\text{H}_2\text{O}$, FeCl_3 . The second method was also the origin of Fe^{+3} ions because it was coming from lithium nitrate and iron (III) nitrate, and the last was a source of Fe^{+3} ions. Then both samples were prepared without Fe^{+2} ions. The vibrating sample magnetometer VSM had been applied to analyze the magnetic properties. The applied model was PPMS VSM Option Release 1.3.6, the quantum design PPMS exhibited in laboratory equipment: an open architecture, variable temperature designed for different measurements. A sample environment is bearing a magnetic field nearly (± 16 tesla) and temperature (1.9-400 K). The main operation of VSM device is the oscillating a sample in the region of detection coil and a synchronized voltage induced. The oscillation head directed vertically to gradiometer pickup coil. The accurate site and vibration intensity controlled by VSM motor through optical linear cipher signal that is read back again during a linear transport. The magnification of induced voltage that is detecting in a VSM unit. The VSM unit uses the cipher signal as a source to a synchronized detection. The interpretation of a cipher signals produced by VSM linear motor transport is related to in-phase and quadrature-phase signals and the magnified voltage created in a pickup coil. The decoding signals are appeared on the VSM software through the CAN bus. This is the main operation of VSM unit

3. Results and discussion

A structural phase of Li-ferrite with the particle size range (46-77 nm), and the presence of spinel cubic phase at lattice parameter ($a=8.328 \text{ \AA}$), space group $\text{Fd}/3\text{m}$ discussed previously [8]. The simulation of XRD-pattern was the key to understand the presence of octahedrons and tetrahedrons within the spinel unit cell. This simulation had been done by using suitable software called Endeavour. The output data of this simulation is shown in Fig.1. The position of atom in a spinel structure depends on structure simulation, as mentioned in Table 1. It well known; the good ferrite is related to the concentration of tetrahedral shape that is must be a twice of octahedral shape.

The magnetic field behavior of lithium ferrite was analyzed at (5 K) for both samples prepared by different methods. The prepared sample by LTSSR undergoes to magnetic field (50 kOe), producing saturation of magnetization of about ($4.763\mu_B$). The magnetic hysteresis loop showed the value of coercive magnetic field of about (1.727 Oe), producing remanence magnetization at ($3\mu_B$). There is a soft hysteresis loop like S-shape with small coercive field, as shown in Fig. 2a. Whereas the hysteresis loop of the sample prepared by MCM method, as shown in Fig. 2b, the loop shape is widen than before at the same applied field with saturation of

magnetization of about ($2.4\mu_B$). It is well known that the magnetic moments take the maximum value as the saturation magnetization goes to maximum. In general, both samples are soft ferrite with the sharp hysteresis loop approaching the same parameter. The magnetic saturation occurs due to the arrangement of magnetic moments the molecules in the structure of principle material. The alignment of magnetic moment is making each molecule act as a tiny magnet within the material. the increasing of magnetic field strength (H) tends to increase a quantity of molecular magnets more and more reaching to a perfect alignment exhibited a maximum flux density. Normally, the increasing of magnetic field strength is happened through the exceeding of electrical current flowing through the coil.

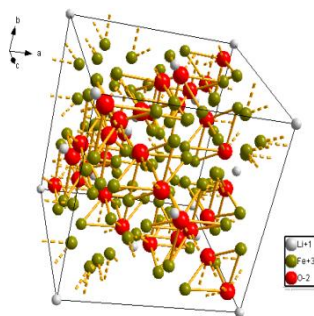


Fig. 1. The simulated unit cell of spinel cubic ferrite.

Table 1. The position of atoms in the spinel structure.

Atom type	x/a	y/b	z/c
Li^{+1}	0	0	0
Fe^{+3}	0.43420	0.06320	0.18680
O^{-2}	0.0692	0.0692	0.0692

The prepared sample of LTSSR showed a maximum magnetic moment of about (0.4 emu) or ($0.4 \times 10^{-3} \text{ JT}^{-1}$) at applied magnetic field (50 kOe), as shown in Fig.3. When the temperature increased to 300 K and the applied magnetic field to (90 kOe) is making a balance in magnetic moments at the same saturation value. That is right because the increasing of magnetic field is the role to save the concentration of tetrahedral and octahedral per unit cell. It is clear that the amount of coercive magnetic field at (90 kOe) is nearly twice of (50 kOe) because of high temperature at 300 K. That is true, because increasing the temperature required increase a coercive magnetic field to remain the ferrite phase. That is agreement with Rinkevich et al [21], they were studied magnetic properties based on ferrite-spinel nanoparticles investigated in temperature range (2-300 K). It is important to remain the tetrahedral and octahedral structure with the same density within the unit cell. As a result of that, the increasing of hysteresis loop area at 300 K tends to make higher magnetic moments of about (0.43 emu). This is a proving to presence of big hysteresis loop at (300 K) and (90 kOe) applied magnetic field. The reason for the remanence magnetization is related to tiny molecular magnets those are completely oriented and the fixed direction of the original magnetized field is a function to a sort of memory.

On the other hand, the effect of different temperature (5,100, and 300 K) and applied magnetic field 50 kOe on the hysteresis loop for the MCM sample is shown in Fig. 4. It is well defined as the temperature increase the area of the loop decrease and the amount of magnetic moments decreased. The high coercive magnetic field is appeared in the hysteresis loop at (5 K) and then decreased as the temperature increased. That is return to high concentration of magnetic moments at low temperature and this concentration will be decreased as the temperature increase with the same applied magnetic field applied. It had been known the shape of the loops is a

function to a soft magnetization but with different area comparing to a loop at (5 K). It is clear that the ferrite material is starting to change toward the paramagnetic material as the temperature increase at (300 K). Then the ferrite material at room temperature has lower magnetization than the low temperature (5 K). Then the ability of Li-ferrite material to save the energy is low, i.e. the Li-ferrite is more beneficial to save the information at low temperature but it is still useful at room temperature before the critical temperature to paramagnetic phase.

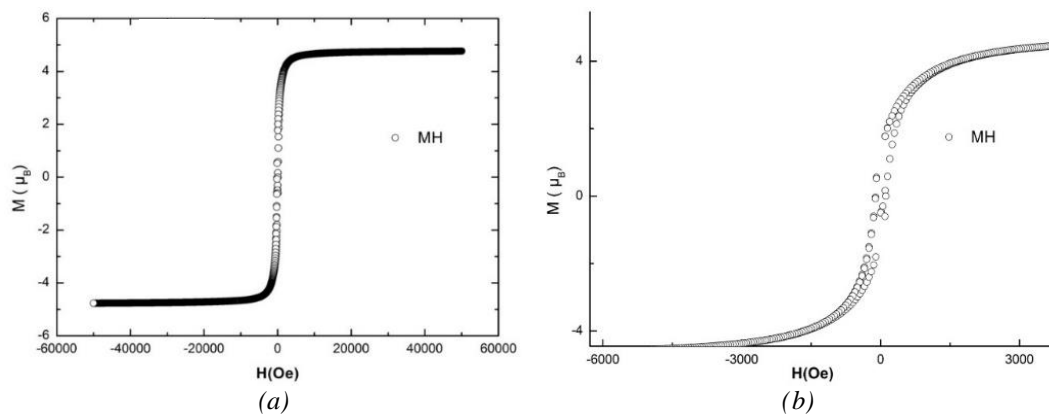


Fig. 2. Magnetization vs magnetic field for $Li_{0.5}Fe_{2.5}O_4$ at 5 K in the sample prepared by (a) LTSSR method (b) MCM method.

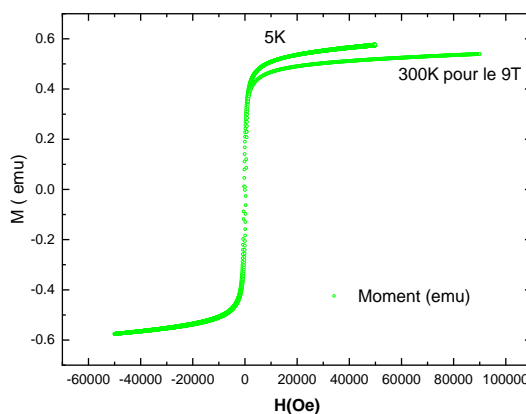


Fig. 3. Magnetic moments vs magnetic field for $Li_{0.5}Fe_{2.5}O_4$ at 5, and 300 K for LTSSR-sample.

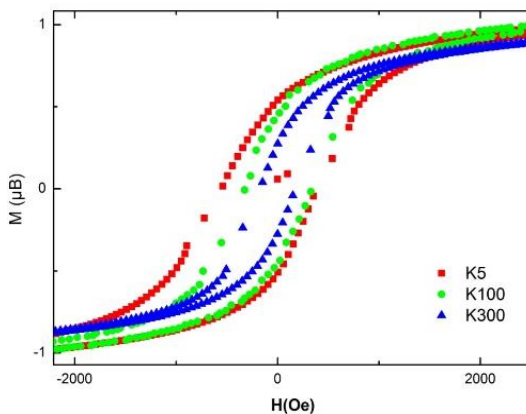


Fig. 4. Magnetization vs magnetic field for $Li_{0.5}Fe_{2.5}O_4$ at different temperature of the two samples.

The hysteresis loops (M–H) of lithium ferrite NPs, as shown in Fig. 4, under a field-cooled (FC) state with an applied field of 500 Oe and various temperatures making a clear coercivity. The inset of above figure showed more details on expanded hysteresis loops near the origin. Then that the hysteresis loops showed “kink or wasp-waisted” property for various temperatures (5,100K), while at 300 K the “wasp-waist” behavior is ignorable. This behavior commonly imputed to the spins canting or disordering at the surface of the nanoparticles that are difficult to stratify along the field direction, this will lead to obtained nanoparticles with an unsaturated magnetization at low temperatures. Many researches have been recorded this loops behavior for magnetic spins at low temperatures (0-100 K) by effect of applied field. The reorientations of spin are responsible for M-H loop affected, which can interpret by definition a domain wall motion and the potential wells created through the directional order of magnetic moments [22], then a consequent tend to change the magnetic behavior of the sample. In addition to appearance the oxidation layer of a soft magnetized may causing this behavior [23]. This property is attributed to a mixture of grain boundaries and different combination of magnetic compounds having various magnetic behavior.

The susceptibility parameter is the key to define the ferrite behavior, then the molar susceptibility and mass susceptibility for both samples as shown in Fig. 5a,b respectively. It is clear that both figures have the same value of susceptibility in the range of (30-32). This is another proof to show there is no difference in the results by changing the preparation method. The decreasing in susceptibility as the temperature increased is true because there is a decreasing of tetrahedral with respect to octahedral per unit cell. This is the key to destroy the ferrite phase by reducing the magnetization in Li-ferrite. So, there is a sharp decreasing in the susceptibility with the temperature before transferring to paramagnetic phase. In the same way, the relation of inverse of molar susceptibility with temperature is a role to save the ferrite behavior before transferring to paramagnetic phase, as shown in Fig. 6 a,b for both ferrite prepared by two methods. That is agreement with Saezpuche et al [24].

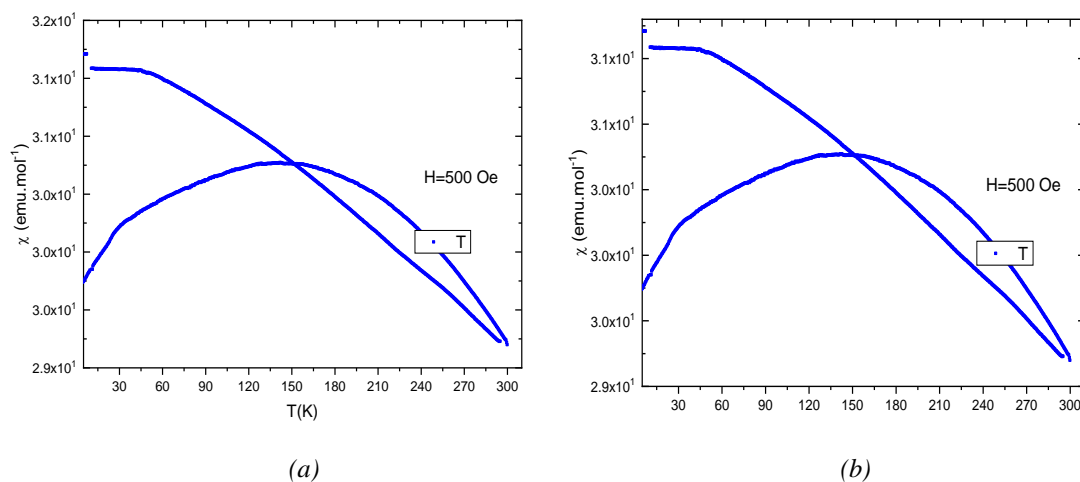


Fig. 5. Field-cooled FC and zero-field-cooled ZFC susceptibilities for $Li_{0.5}Fe_{2.5}O_4$ at 500 Oe of the sample prepared by (a) LTSSR method and (b) MCM method.

This behavior caused by interchange a coupling between a ferromagnetic sub-lattice, the interchange coupling between dissemble antiferromagnetic sub-lattices, interchange a coupling through ferromagnetic/dissemble antiferromagnetic and paramagnetic sub-lattices, inequivalent of spin and orbital moments, and interstitial coupling between ferromagnetic and antiferromagnetic phases [18-20].

The magnetic behavior of two samples lithium ferrite NPs those mentioned by LTSSR and MCM methods, zero field cooled (ZFC) and field cooled (FC) magnetization curves were obtained in the temperature range (5-300 K) at a constant magnetic field 500 Oe. The ZFC and FC magnetization curves at the applied magnetic field (500 Oe) were shown in Fig. 5a,b respectively. The susceptibility parameter (χ) decreased from the maximum value about ($31.5 \text{ emu mol}^{-1}$) with increasing temperature until it reach to the lower value about ($29.2 \text{ emu mol}^{-1}$) at (300 K). Then

increase the susceptibility value with decreasing of temperature until reach to ($30.9 \text{ emu mol}^{-1}$) at about (150 K) and then decreasing to ($30.1 \text{ emu}\cdot\text{mol}^{-1}$) at about (5 K).

For individual nanoparticle, ZFC magnetic curve showed increasing as a function of temperature due to a limited thermal fluctuation may causes the alignment magnetization towards the applied field direction. At a certain temperature called a blocking temperature T_B , the thermal energy is more than the anisotropy energy that tend to the random thermal fluctuations, the last one is the reason to decrease a magnetization decreases as temperature increased. The particle size distribution is producing a broad peak observation instead of a sharp peak near T_B . The FC curve showed a continuous decreasing of magnetization as a function of temperature raising. In this case, the magnetization must be directed along the magnetic field, so that the exceeding in a thermal fluctuation at high temperature tend to reduce the component of magnetization along the direction of H

The irreversibility in ZFC and FC curves occurred at (155 K) and (165 K) [25,26]. This peak point is known as the blocking temperature (T_b); after peak point the magnetization tends to fall rapidly. The sudden decrease in the magnetization of ZFC after T_b is attributed to spin glass behavior of strongly-interacting particles in a magnetic system [27]. This suggested that the increasing in cooling field the ZFC-FC cycles becomes broader, and T_b and T_{irr} shift towards lower temperatures. This behavior typically identifies the super-Paramagnetism below T_{irr} and strong dipolar interactions among the particles [28].

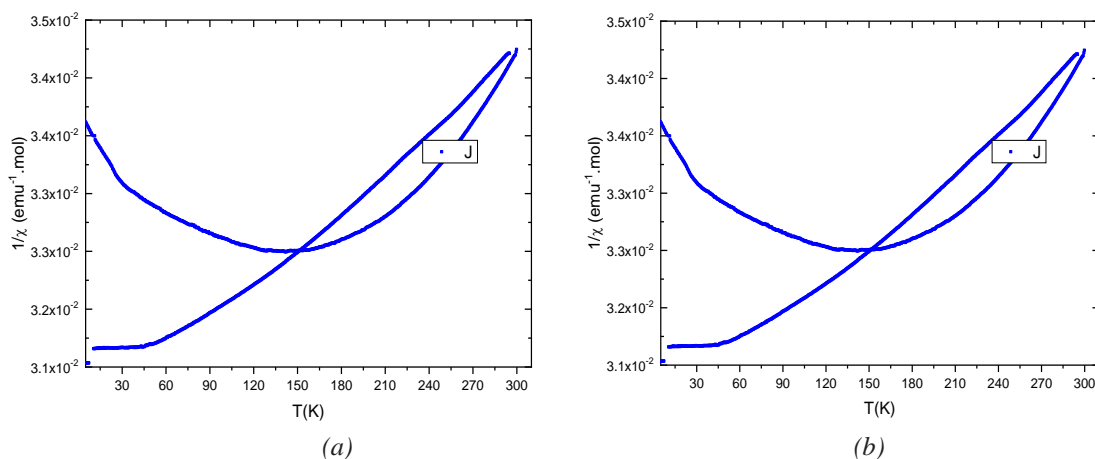


Fig. 6. Inverse of molar susceptibility vs temperature for $\text{Li}_{0.5}\text{Fe}_{2.5}\text{O}_4$ at 500 Oe for the sample prepared (a) LTSSR method (b) MCM method.

4. Conclusions

The magnetic behavior of $\text{Li}_{0.5}\text{Fe}_{2.5}\text{O}_4$ nanoparticles of ferrite-spinel structure had been studied in details. The hysteresis loop curve for two samples prepared by different method LTSTR, and MCM methods were obtained and show same behavior. It can be concluded that the magnetic phase introduced is ordered ferrimagnetic with soft case and partially it had superparamagnetic properties. The presence of nano-sized particles in the size (46-77 nm), which cause the superparamagnetic properties. The coercive magnetic field of nanoparticle is increasing sharply as the temperature increased. The area of hysteresis loop showed the inverse behavior with temperature increase that means the amount of energy storage is decreased also. The reducing of hysteresis is a function toward the paramagnetic behavior. This is another proof of soft ferrite presented of nanoparticles Li-ferrite. The relation between magnetization and temperature under Zero-field-cooled ZFC and field-cooled FC modes were obtained.

Acknowledgments

The research was carried out under the supervision Prof. Dr. B. Elouadi, from La Rochelle University / France who helped us to perform all the magnetic measurements. These measurements were done in France under the sponsorship of La Rochelle University. Much thanks also to the France embassy in Baghdad, for completion the residence and travel requirements to France in order to complete all the results and analysis.

References

- [1] D. Gingasu, I. Mindru, L. Patron, and S. Stoleriu; Synthesis of lithium ferrites from polymetallic carboxylates, *J. Serb. Chem. Soc.* 73 (10), pp. 979-988, (2008). <https://doi.org/10.2298/JSC0810979G>
- [2] E. Wolska, P. Piszora, W. Nowicki, J. Darul; Vibrational spectra of lithium ferrites: infrared spectroscopic studies of Mn-substituted LiFe₅O₈, *International Journal of Inorganic Materials*, 3, pp. 503-507, (2001). [https://doi.org/10.1016/S1466-6049\(01\)00069-1](https://doi.org/10.1016/S1466-6049(01)00069-1)
- [3] M.N. Iliev, V.G. Ivanov, N.D. Todorov, V. Marinova, M.V. Abrashev, R. Petrova, Y.-Q. Wang, and A. P. Litvinchuk; Lattice dynamics of the α and β phases of LiFe₅O₈, *Physical Review B* 83, pp. 1741111-7, (2011). <https://doi.org/10.1103/PhysRevB.83.174111>
- [4] S. Verma and P.A. Joy; Magnetic properties of superparamagnetic lithium ferrite nanoparticles, *J. of APPLIED PHYSICS* 98, pp. 1243121-9, (2005). <https://doi.org/10.1063/1.2149493>
- [5] H.M. Widatallah, C. Johnson, J.F. Marco, F.J. Berry, A.M. Gismelseed, E. Jartych, J.F. Marco, F.S. Gard, and M. Pekala; Synthesis and cation distribution of copper-substituted spinel-related lithium ferrite, *J. of Physics and Chemistry of Solids* 67, pp.1817-1822, (2006). <https://doi.org/10.1016/j.jpcs.2006.04.003>
- [6] S. Dey, A. Roy, D. Das, and J. Ghose; Preparation and characterization of nanocrystalline disordered lithium ferrite by citrate precursor method, *J. of Magnetism and Magnetic Materials* 270, pp. 224-229, (2004). <https://doi.org/10.1016/j.jmmm.2003.08.024>
- [7] A. Ahniyaz, T. Fujiwara, S.-W. Song, and M. Yoshimura; Low temperature preparation of β -LiFe₅O₈ fine particles by hydrothermal ball milling, *Solid State Ionics* 151, pp. 419-423, (2002). [https://doi.org/10.1016/S0167-2738\(02\)00548-9](https://doi.org/10.1016/S0167-2738(02)00548-9)
- [8] I.M. Abdulmajeed, E.K. AL-Shakarchi, M.H. Al-Dharob, and Brahim Elouadi; Preparation of Nanoparticle Li-Ferrite Materials by Different Chemical Method, *European International Journal of Science and Technology*, 4(2), pp. 69-76, (2015).
- [9] X. Yu, C. Zhang, Z. Luo, T. Zhang, J. Liu, J. Li, Y. Zuo, J.J. Biendicho, J. Llorca, J. Arbiol, J.R. Morante, and A. Cabot; A low temperature solid state reaction to produce hollow Mn_xFe_{3-x}O₄ nanoparticles as anode for lithium-ion batteries Cabot; *Nano Energy*, accepted for publishing, October (2019). <https://doi.org/10.1016/j.nanoen.2019.104199>
- [10] Gh.R. Amiri, M.H. Yousefi, M.R. Aboulhassani, M.H. Keshavarz, D. Shahbazi, S. Fatahian, and M. Alahi; Radar Absorption of Ni_{0.7}Zn_{0.3}Fe₂O₄ Nanoparticles; *Digest J. of Nanomaterials and Biostructures*, 5, 3, pp. 719-725, (2010).
- [11] R. Qin, F. Li, W. Jiang, and L. Liu; Salt-assisted Low Temperature Solid State Synthesis of High Surface Area CoFe₂O₄ Nanoparticles; *J. Mater. Sci. Technol.*, 25, 1, pp. 69-72, (2009).
- [12] N.G. Jovic, A.S. Masadeh, A.S. Kremenovic, B.V. Antic, J.L. Blanusa, N.D. Cvjeticanin, G.F. Goya, M.V. Antisari, and E.S. Bozin; Effects of Thermal Annealing on Structural and Magnetic Properties of Lithium Ferrite Nanoparticles; *J. Phys. Chem. C*, 113, pp. 20559-20567, (2009). <https://doi.org/10.1021/jp907559y>
- [13] M. Sugimoto; The past, present, and future of ferrites; *J. Material Ceram. Soc.*, 82, pp. 269-279, (1999). <https://doi.org/10.1111/j.1551-2916.1999.tb20058.x>
- [14] E.F. Kneller, R. Hawig; The exchange-spring magnet: a new material principle for permanent magnets; *IEEE Trans. Magn.*, 27(4), pp. 3588-3560, (1991). <https://doi.org/10.1109/20.102931>
- [15] F. Song, X. Shen, M. Liu, J. Xiang; Magnetic hard/soft nanocomposite ferrite aligned hollow microfibers and remanence enhancement; *J. Colloid. Interf. Sci.*, 354, pp. 413-416, (2011). <https://doi.org/10.1016/j.jcis.2010.11.020>

- [16] Q. A. Pankhurst, J. Connolly, S. K. Jones, and J. Dobson; Applications of magnetic nanoparticles in biomedicine, *J. Phys. D* 36, pp. R167-R181, (2003).
<https://doi.org/10.1088/0022-3727/36/13/201>
- [17] M. Shinkai, Functional Magnetic Particles for Medical Application, *J. Biosci. Bioeng.* 94(6), pp.606-613, (2002).
- [18] A. Kumar, S.M. Yusuf; The phenomenon of negative magnetization and its implications; *Physics Reports Volume 556*, pp.1-34, (2015). <https://doi.org/10.1016/j.physrep.2014.10.003>
- [19] M. Hase, V.Yu. Pomjakushin, V. Sikolenko, L. Keller, H. Luetkens, A. Donni, and H. Kitazawa; Negative magnetization of $\text{Li}_2\text{Ni}_2\text{Mo}_3\text{O}_{12}$ having a spin system composed of distorted honeycomb lattices and linear chains; *Phys. Rev. B* 84, pp. 1044021-8, (2011).
<https://doi.org/10.1103/PhysRevB.84.104402>
- [20] C. Li, T. Yan, C. Chakrabarti, R. Zhang, X. Chen, Q. Fu, S. Yuan, and G.O. Barasa; Negative magnetization and the sign reversal of exchange bias field in $\text{Co}(\text{Cr}_{1-x}\text{Mn}_x)_2\text{O}_4$ ($0 \leq x \leq 0.6$); *J. Applied Physics* 123, pp. 0939021-6, (2018). <https://doi.org/10.1063/1.5009404>
- [21] A.B. Rinkevich, A.V. Korolev, M.I. Samoylovich, S.M. Klescheva, D.V. Perov; Magnetic properties of nanocomposites based on opal matrices with embedded ferrite-spinel nanoparticles, *Journal of Magnetism and Magnetic Materials*, 399, pp. 216-220, (2016).
<https://doi.org/10.1016/j.jmmm.2015.09.068>
- [22] Q. Gao, G. Hong, J. Ni, W. Wang, J. Tang, and J. He; Uniaxial anisotropy and novel magnetic behaviors of CoFe_2O_4 nanoparticles prepared in a magnetic field; *J. Appl. Phys.* 105, pp. 07A5161-3, (2009). <https://doi.org/10.1063/1.3072019>
- [23] S. Heisz, G. Hilscher; The origin of graduated demagnetization curves of NdFeB magnets; *J. Magn. Magn. Mater.*, 67, pp. 20-28, (1987). [https://doi.org/10.1016/0304-8853\(87\)90714-1](https://doi.org/10.1016/0304-8853(87)90714-1)
- [24] R.S. Puche, M. J. T. Fernandez, V. B. Gutierrez, R. Gomez, V. Marquina, M.L. Marquina, J.L.P. Mazariego, R. Ridaura; Ferrites nanoparticles MFe_2O_4 ($\text{M} = \text{Ni}$ and Zn): hydrothermal synthesis and magnetic properties, *Bol. Soc. Esp. Ceram. V.*, 47(3), pp. 133-137, (2008)
<https://doi.org/10.3989/cyv.2008.v47.i3.189>
- [25] Y. Imry, S.-K Ma; Random-Field Instability of the Ordered State of Continuous Symmetry *Phys. Rev. Lett.* 35, pp. 1399-1401(1975). <https://doi.org/10.1103/PhysRevLett.35.1399>
- [26] C.G. Shull, W.A. Strauser, and E.O. Wollan; Neutron Diffraction by Paramagnetic and Antiferromagnetic Substances; *Phys. Rev.* 83(2), pp. 333-345, (1951).
<https://doi.org/10.1103/PhysRev.83.333>
- [27] B. Ghosh, S. Kumar, A. Poddar, C. Mazumdar, S. Banerjee, V.R. Reddy, and A. Gupta; Spin glasslike behavior and magnetic enhancement in nanosized Ni-Zn ferrite system; *J. Appl. Phys.*, 108, pp. 0343071-8, (2010). <https://doi.org/10.1063/1.3456174>
- [28] A.J. Rondinone, A.C.S. Samia, and Z.J. Zhang; Superparamagnetic Relaxation and Magnetic Anisotropy Energy Distribution in CoFe_2O_4 Spinel Ferrite Nanocrystallites; *J. Phys. Chem. B*, 103, pp. 6876-6880, (1999). <https://doi.org/10.1021/jp9912307>